This document was prepared in conjunction with work accomplished under Contract No. DE-AC09-96SR18500 with the U.S. Department of Energy.

WSRC-STI-2007-00571

TRITIUM AGING EFFECTS ON THE FRACTURE TOUGHNESS PROPERTIES OF FORGED STAINLESS STEEL*

Michael J. Morgan

Savannah River National Laboratory
Aiken, SC 29808

803-725-2245
michael.morgan@srnl.doe.gov

A paper proposed for publication in the Conference Proceedings

Materials Innovations in an Emerging Hydrogen Economy

February 24-27, 2008
Cocoa Beach, Florida

TRITIUM AGING EFFECTS ON THE FRACTURE TOUGHNESS PROPERTIES OF FORGED STAINLESS STEEL

Michael J. Morgan
Savannah River National Laboratory
Aiken, SC, USA

ABSTRACT

The fracture toughness properties of Type 21-6-9 stainless steel were measured for forgings in the unexposed, hydrogen-exposed, and tritium-exposed-and-aged conditions. Fracture toughness samples were cut from conventionally-forged and high-energy-rate-forged forward-extruded cylinders and mechanically tested at room temperature using ASTM fracture-toughness testing procedures. Some of the samples were exposed to either hydrogen or tritium gas (340 MPa, 623 K) prior to testing. Tritium-exposed samples were aged for up to seven years and tested periodically in order to measure the effect on fracture toughness of ^{3}He from radioactive tritium decay. The results show that hydrogen-exposed and tritium-exposed samples had lower fracture- toughness values than unexposed samples and that fracture toughness decreased with increasing decay ^{3}He content. Forged steels were more resistant to the embrittling effects of tritium and decay ^{3}He than annealed steels, although their fracture-toughness properties depended on the degree of sensitization that occurred during processing. The fracture process was dominated by microvoid nucleation, growth and coalescence; however, the size and spacing of microvoids on the fracture surfaces were affected by hydrogen and tritium with the lowest-toughness samples having the smallest microvoids and finest spacing.

INTRODUCTION

Tritium and its decay product, helium, change the structural properties of stainless steels and make them more susceptible to cracking. Tritium embrittlement is an enhanced form of hydrogen embrittlement because of the presence of ^{3}He from tritium decay which nucleates as nanometer-sized bubbles on dislocations, grain boundaries, and other microstructural defects. Steels with decay helium bubble microstructures are hardened and less able to deform plastically and become more susceptible to embrittlement by hydrogen and its isotopes (1-7).

Tritium is stored at Savannah River in stainless steel reservoirs constructed from Types 304L, 316L, and 21-6-9 stainless steel forgings. Material and forging specifications have been developed for optimal material compatibility with tritium. These specifications cover composition, tensile properties, and select microstructural characteristics like grain size, flow line orientation, inclusion content, and ferrite distribution and content. For many years, the forming process of choice for reservoir manufacturing was high-energy-rate forging (HERF), principally because the DOE forging facility owned only HERF hammers. Today, some reservoir forgings are being made that use a conventional, more common process known as press forging (PF or CF) (1). One of the chief differences between the two forging processes is strain rate: Conventional hydraulic or mechanical forging presses deform the metal at 120-240 cm/s, about ten-fold slower than the HERF process.

The material specifications continue to provide successful stockpile performance by ensuring that the two forging processes produce similar reservoir microstructures. However a detailed comparison of the effects of tritium on the fracture toughness properties of steels having similar composition, grain size, and mechanical properties, but produced by different forming processes, has not been conducted until now. Furthermore, fracture toughness properties are needed for designing and establishing longer tritium reservoir lifetimes, ranking materials and their behavior, and, potentially, for qualifying new forging vendors or processes.

The purpose of this study was to measure and compare the fracture toughness properties of Type 21-6-9 stainless steel for high-energy-rate and conventional forgings in the unexposed, hydrogen-exposed and tritium-exposed-and-aged conditions.

EXPERIMENTAL PROCEDURE

Three heats of Type 21-6-9 stainless steel were used in this study. The compositions are listed in Table I. The steel was supplied in the form of six-inch long by 1.5 inch diameter forward extruded cylindrical forgings (Type L109) either high-energy-rate forged or conventionally forged. The forgings were produced so that the mechanical properties (yield strength, ultimate strength, hardness profile, and elongation), grain size, and inclusion and ferrite content and distribution were similar to reservoir steels. Two heats of CF stainless steel were used. One heat had a yield strength of 685 MPa, which was similar to the yield strength of the HERF heat, 722 MPa. The other CF heat had a yield strength of 600 MPa and was used to determine the effect of yield strength on toughness by comparison with the 685 MPa CF heat. The HERF heat was chosen from the same lot of forgings used in previous tritium studies at the Savannah River National Laboratory (3, 7). The mechanical properties of the forgings are shown in Table II.

Table I. Compositions of Stainless Steel Forgings, Plates and Weld Filler Wires (Weight %)

Material	Forging	Sample ID	Cr	Ni	Mn	P	Si	C	S	N	O	Al
21-6-9 HERF*	A4582	F97-X	19.4	6.4	8.5	0.021	0.33	0.04	<.001	0.28	0.0022	<.001
21-6-9 CF**	B7073	H94-X	19.1	6.7	9.9	0.01	0.41	0.03	0.004	0.28	0.001	0.005
21-6-9 CF**	B6275	F9-X	19.3	6.7	9.9	0.01	0.38	0.03	0.001	0.28	0.002	0.004

*High-Energy-Rate Forged
**Conventionally Forged
Manufacturers' supplied compositions.

Table II. Mechanical Properties and Grain Size

Sample ID	Yield Strength MPa	Ultimate Strength MPa	% EL	Grain Size
F9 (CF)	600	906	48.3	10/7; 7 < 5%
H94 (CF)	685	960	44.3	10/7; 7 < 5%
F97 (HERF)	722	961	37.6	5/3

Arc-shaped fracture-mechanics specimens having the shape and dimensions shown in Figure 1 were fabricated from the forgings and oriented so that the cracks would propagate across the forging flow lines in the radial direction (C-R). The samples were fatigue-cracked so that the crack-length to sample-width ratio was between 0.4 and 0.6. The size of the samples was chosen to be as large as

possible to maximize constraint but thin enough to saturate the samples with hydrogen or tritium at temperatures that would not alter the microstructure.

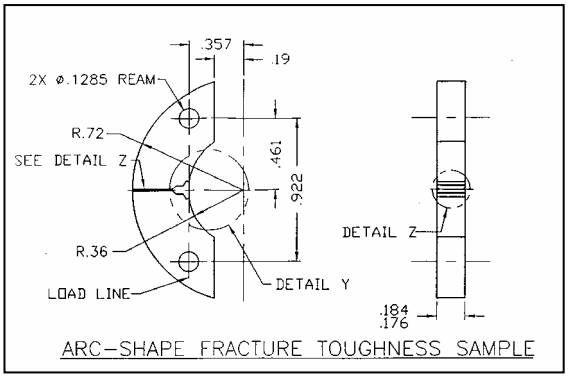

Figure 1. Shape and Dimensions in Inches of Fracture Toughness Sample.

Three sets of samples were prepared from each forging: Unexposed, hydrogen-exposed, and tritium-exposed-and-aged. Some of the unexposed samples were heat treated prior to testing as described below. Hydrogen-exposed samples were prepared by equilibrating samples with hydrogen gas at either 34 MPa or 69 MPa at 623 K for three weeks. Tritium exposures were conducted at 34 MPa 623 K. The exposures were designed to saturate the samples throughout the thickness. Samples were stored at 233 K prior to testing to minimize hydrogen or tritium losses from off-gassing. Tritium-samples were stored for up to seven years prior to testing to build in helium from tritium decay. Tritium-charged samples were analyzed for decay-helium content by isotope-dilution gas mass spectrometry following vaporization in a resistance-heated graphite crucible in a vacuum furnace. The helium content on the date of each test was back-calculated from the measured values by accounting for tritium decay and ranged from 90-800 atomic parts per million (appm).

J-integral tests were conducted at room temperature in air using a screw-driven testing machine and a crosshead speed of 0.002 mm/s. while recording load, load-line displacement with a gage clipped to the crack mouth, and crack length. Crack length was monitored using an alternating DC potential drop system and guidelines described in ASTM E647-95 (8). The J-Integral versus crack length increase (J vs. da) curves were constructed from the data using ASTM E1820-99 (9). The J_Q value is defined as the material fracture toughness and was obtained from the intercept of an offset from the crack tip blunting line with the J-da curve. For this study, the crack tip blunting line for the weldments was assumed to be the same as the blunting line for the base metal and was calculated from the yield strength and ultimate strength of the base metal per the ASTM 1820 procedure.

Material microstructures were characterized using standard metallographic techniques.

RESULTS

A typical load-displacement record from a fracture toughness test for forged stainless steel and the corresponding DC potential drop signal for crack length monitoring is shown in Figure 2. The J-integral fracture toughness data were determined from these load-displacement-crack length records and plots of the J-Integral versus the change in crack length (da), per ASTM 1820. Figure 3 shows a comparison between the typical J-da plots for the unexposed CF and HERF heats of steels. Note that the CF heat had higher fracture-toughness values than the HERF heat. For forgings of yield strength of 685 MPa, the CF heats had an average fracture toughness value of 2115 lbs-in (six tests) while the HERF heats averaged 1203 lbs-in (two tests). This was a surprising result, so a detailed examination of the fracture modes of both heats was conducted.

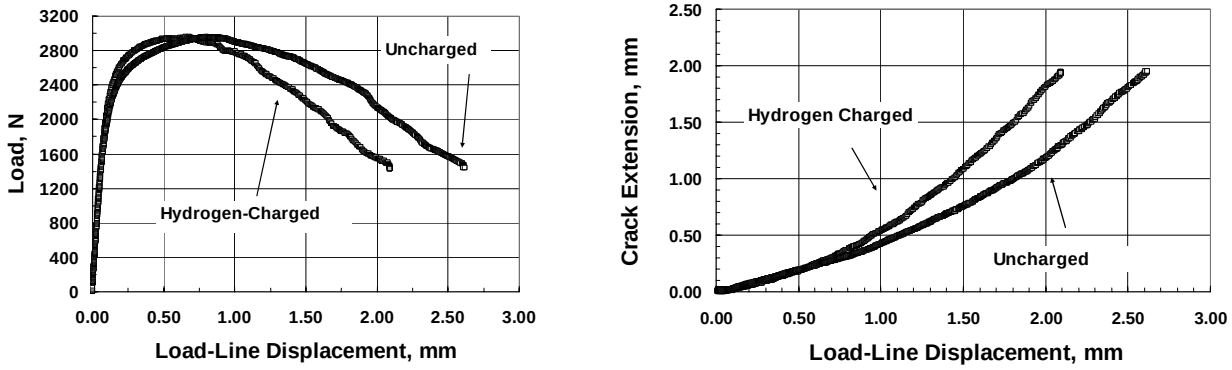

Figure 2. Typical Load-Displacement (left) and Potential-Drop-Crack-Length-Measurement (right) Records Acquired During Fracture Toughness Test of Forged Stainless Steel.

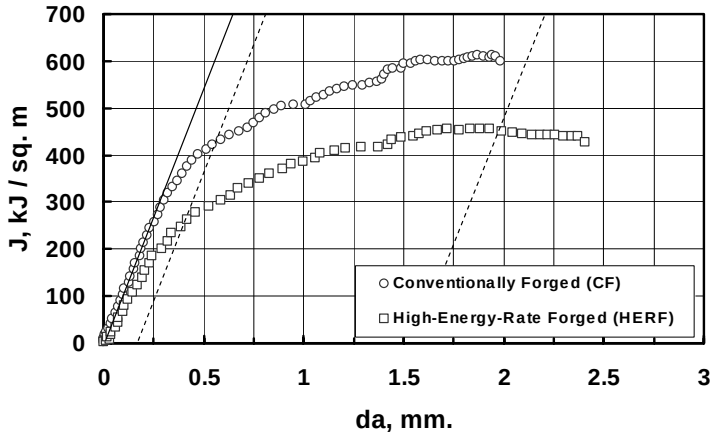

Figure 3. Comparison of the J-Integral (J) vs. Change-in-Crack Length (da) Curves for Conventionally-Forged and High-Energy-Rate-Forged Type 21-6-9 stainless steel in the As-Received Condition.

The fracture mode of both forgings was by the microvoid nucleation and growth process (Figure 4). Microvoids nucleate at nonmetallic inclusions in the steel (sulfides, oxides, etc) and grow under strain until they coalesce at fracture (10). While the CF heats had a fairly uniform microvoid size distribution on the fracture surface, the HERF steel fracture surface had a bimodal distribution of microvoids with large microvoids surrounded by clusters of fine microvoids.

The microstructures of the forged steels are shown in Figure 5. The HERF microstructure was significantly different than the CF microstructures. The HERF heat had a larger grain size and, more importantly, it appeared to have been sensitized. Fracture toughness tends to decrease with increasing grain size but the difference in toughness between the HERF and CF steels seemed to be too large to be explained by just the grain size difference, particularly since the fracture mode was dimpled rupture. The cluster of fine microvoids observed on the HERF fracture surfaces suggest association with carbides (10) and the most likely cause of the fracture toughness difference between the CF and HERF steels.

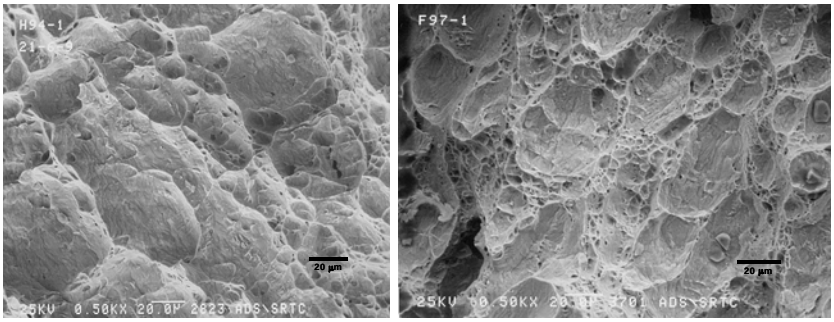

Figure 4. Comparison of the Fracture Appearance of the Unexposed Heats of Type 21-6-9 Stainless Steel (a) Conventionally Forged,; and (b) HERF. Arrows Indicate Crack Propagation Direction.

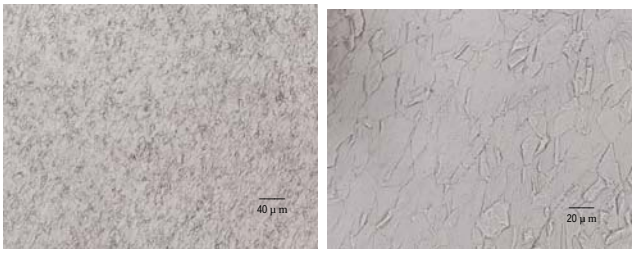

(a)

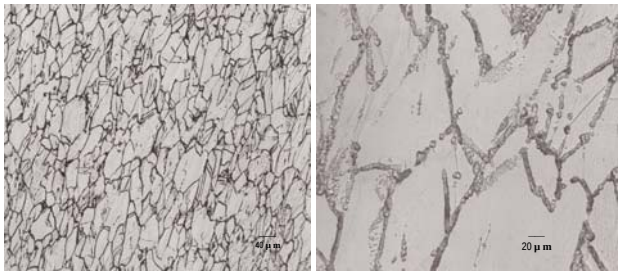

(b)

Figure 5. Typical Microstructures of Forged Type 21-6-9 Stainless Steel (Oxalic Acid Etch, 90 s): (a) Conventionally Forged; and, (b) High-Energy-Rate Forged.

In order to test this hypothesis, the two forgings were heat treated for five minutes at 650°C, the temperature at which grain boundary carbides will precipitate in short times. Fracture-toughness tests were then conducted and the results are shown in Figure 6. Note that the fracture-toughness values of both heats were reduced after the heat treatment and that the conventionally-forged alloy fracture toughness was reduced to the value of the as-received HERF alloy. The fracture modes of the heat-treated alloys are shown in Figure 7 and they both show a bimodal microvoid distribution, with clusters of fine microvoids mixed in with the larger microvoids.

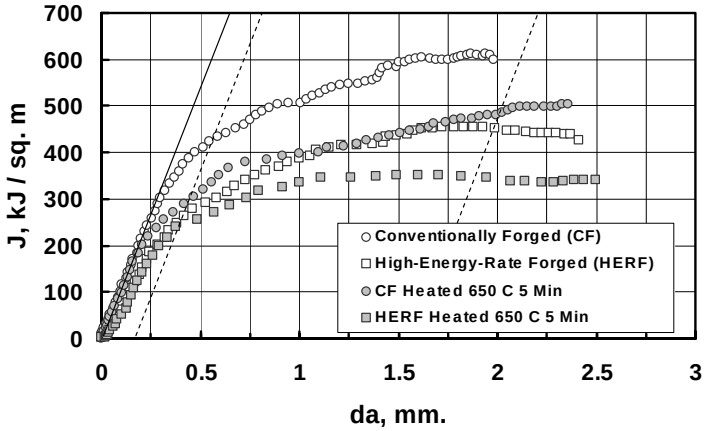

Figure 6**.** J-Integral (J) vs. Change-in-Crack Length (da) Behavior for As-Received and Heat-Treated Type 21-6-9 Stainless Steels.

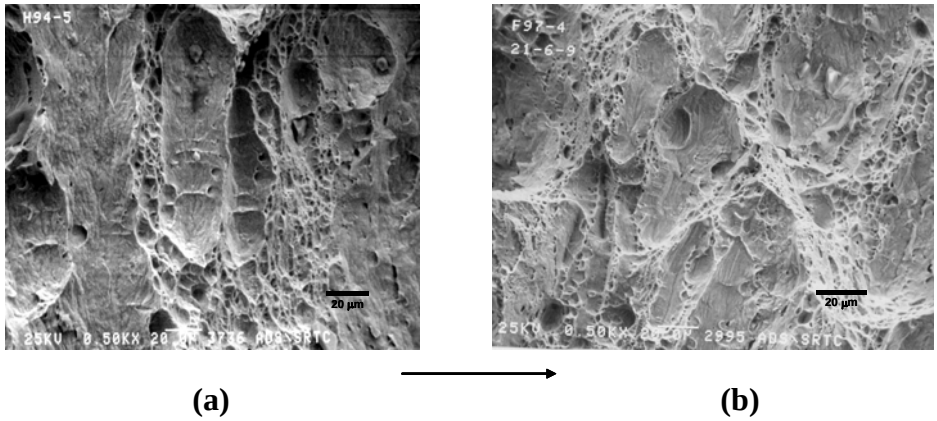

Figure 7. Fracture Appearance of Steels Heat Treated for Five Minutes at 650°C: (a) Conventionally Forged and (b) HERF. Arrow Indicates Crack Propagation Direction.

A second purpose of this study was to investigate the effect of hydrogen and tritium exposures on the properties of Type 21-6-9 stainless steel. Figure 8 shows the large fracture toughness reductions after hydrogen exposures of 34 MPa and 69 MPa. The fracture appearance of the hydrogen-exposed alloys is shown in Figure 9. By comparison with Figure 4, the effect of hydrogen is dramatic in that the size of the microvoids on the fracture surface is greatly reduced.

The effect of tritium and decay helium on these steels was studied by aging the steels after tritium exposure and then testing periodically. Figure 10 shows that the change in J-da behavior for unexposed, hydrogen-exposed and tritium-exposed-and-aged conventionally forged steel. Note the reduction in the J-da behavior for the tritium-exposed-and-aged sample when compared to a similar sample exposed to hydrogen gas. The fracture toughness is reduced even more because of decay helium. As the samples were aged, fracture toughness values decreased even more with increasing decay helium content. This is shown in Figure 11.

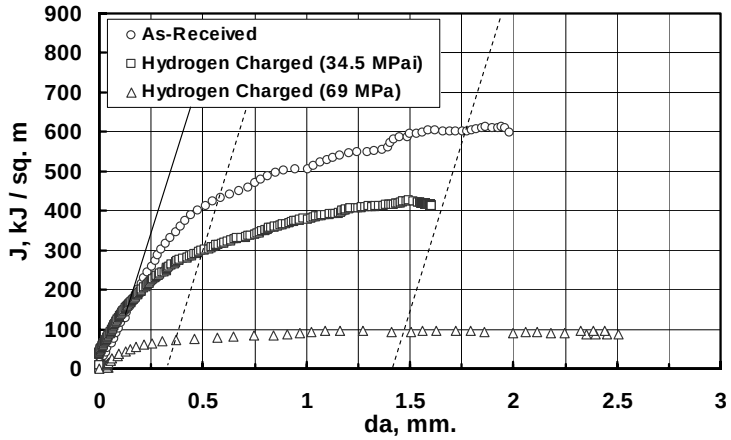

Figure 8. Effect of Hydrogen on the J-da Behavior for Conventionally Forged Type 21-6-9 Stainless Steels. Hydrogen Exposures Were Conducted at 34 MPa and 69 MPa.

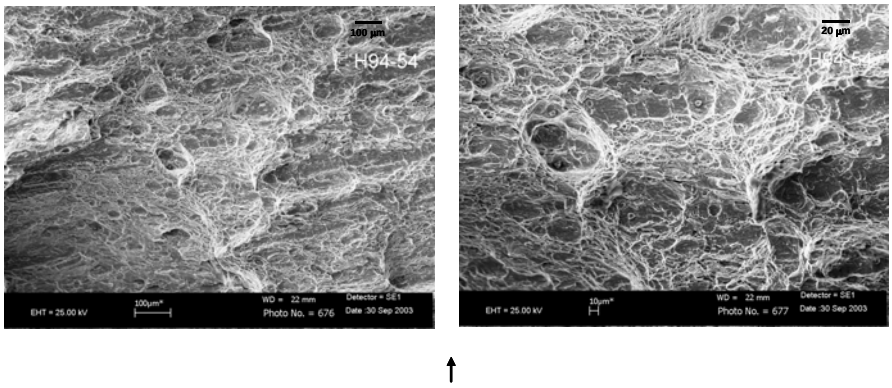

(a) **(b)**

Figure 9. Fracture Appearance of Conventionally Forged Type 21-6-9 Steel after Exposure to Hydrogen Gas (34MPa): (a) 100 X (b) 500X. Arrow Indicates Direction of Crack Propagation.

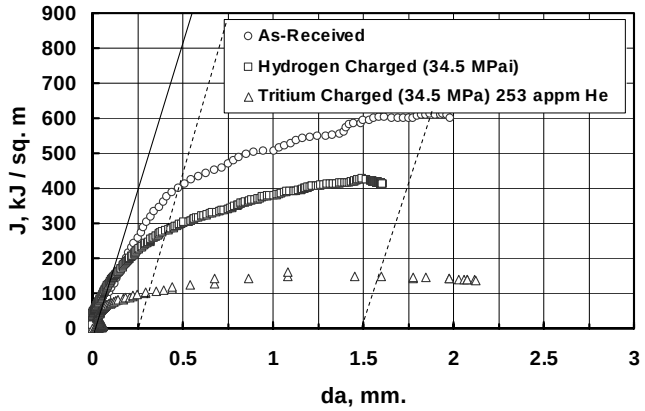

Figure 10. Effect of Hydrogen, Tritium and Decay Helium on the J-Integral (J) vs. Change-in-Crack-Length (da) Behavior for Conventionally Forged Type 21-6-9 Stainless Steels.

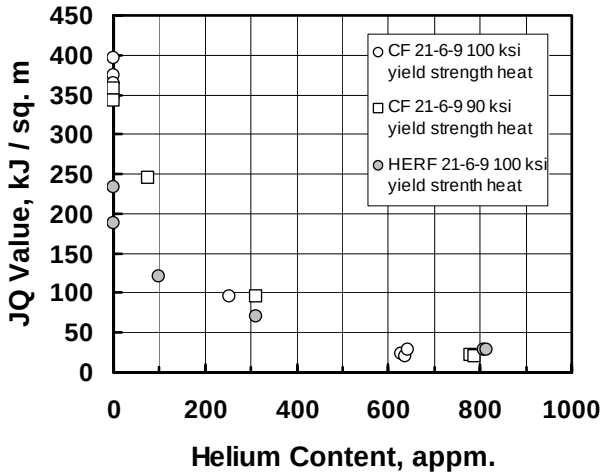

Figure 11. Effect of Decay Helium Content on the J-Integral Fracture Toughness Values of Conventionally Forged and High-Energy-Rate-Forged Type 21-6-9 Stainless Steel.

Note the two conventionally forged heats had similar fracture toughness values as a function of helium content. The yield strength difference between these two heats (600 vs. 685 MPa) had little effect on fracture toughness. On the other hand, the HERF steel (722 MPa yield strength) had fracture toughness values that were lower prior to aging, most likely due to the sensitized microstructure. Note also that the toughness values of all heats converged to similar values at high levels of decay helium.

The fracture modes of the tritium-exposed alloys are shown in Figures 12 and 13 for the CF steels and in Figure 14 for the HERF steels. The fracture mode was still microvoid coalescence but now the voids were even smaller (~1 um) than those in the hydrogen-exposed alloys.

One final test was conducted on a heat treated sample to elucidate the effect of heat treatment and sensitization on the fracture behavior of this steel. A CF sample was heated for 24 hours at 650°C to see if the fracture mode would continue to change with an even larger amount of carbide precipitation. Note in Figure 15-a this heavily sensitized steel has a fracture appearance that is completely dominated by small microvoids associated with carbides. The bimodal distribution of microvoids like those in Figure 7 has been eliminated. In fact, the fracture appearance is remarkably similar to that of the tritium-exposed-and-aged steels albeit at a different magnification (Figure 15-b). It appears that carbides in the microstructure affect the fracture mode in a similar manner as the decay helium bubbles but on a different scale.

DISCUSSION

The results of this study provide a number of important insights into the cracking behavior and fracture toughness properties of Type 21-6-9 stainless steel forgings. First of all, the study indicates that it is difficult to directly compare the fracture toughness properties of material made by different forging processes because the degree of sensitization can vary from one forging process to the other or maybe even one forging to another. In this study, the high-energy-rate-forged steel was chosen from the lot of forgings that had been used in earlier studies at Savannah River National Laboratory so that comparisons could be made to those studies (3, 7). This heat apparently had been sensitized during the forging process and the sensitization caused a reduction in fracture toughness (Figure 3).

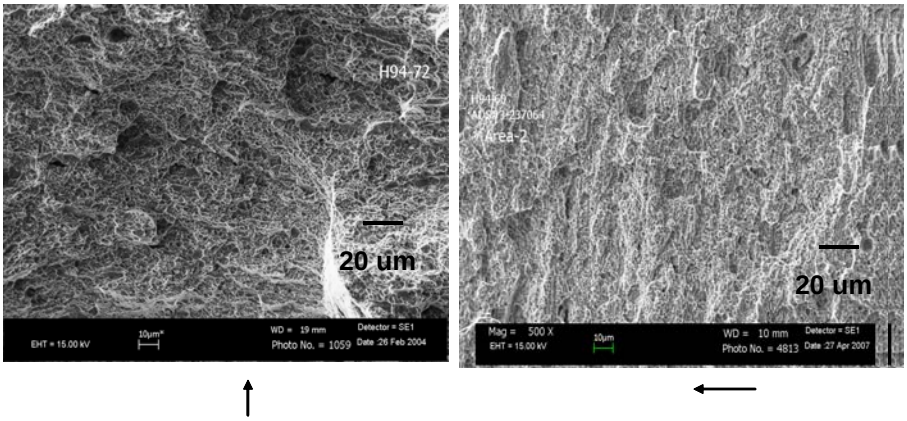

Figure 12. Fracture Appearance of Conventionally Forged Type 21-6-9 Steel after Exposure to Tritium Gas (5000 psi, 350°C) and Aged for Helium Build-In from Tritium Decay: (a) 253 appm helium; and (b) 627 appm helium. Arrows Indicate Direction of Crack Propagation.

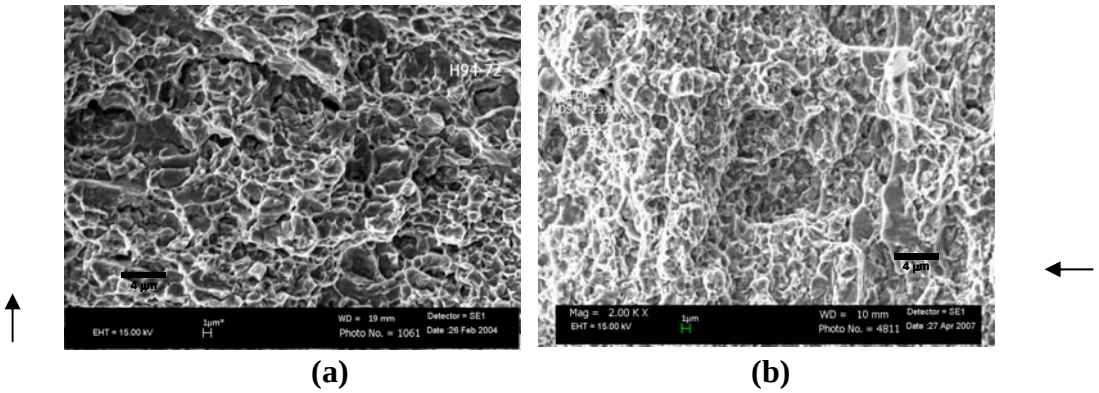

Figure 13. High Magnification Image of Fracture Appearance of Conventionally Forged Type 21-6-9 Steel after Exposure to Tritium Gas (5000 psi, 350°C) and Aging until Decay Helium Content Was: (a) 253 appm; and (b) 627 appm. Arrows Indicate Direction of Crack Propagation.

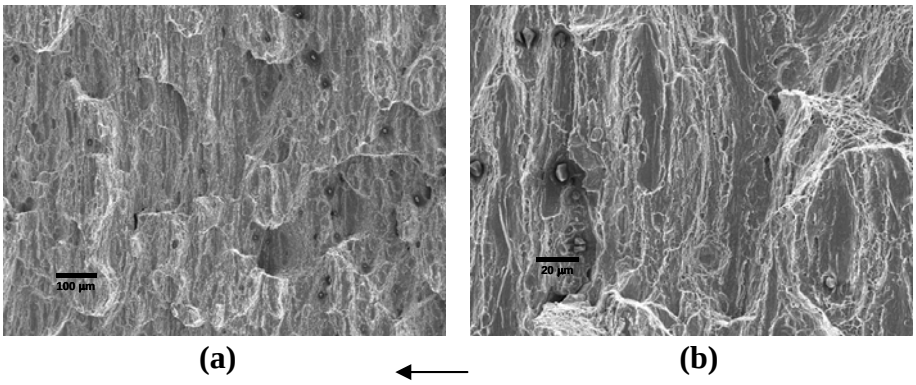

Figure 14. Fracture Appearance of HERF Type 21-6-9 Steel after Exposure to Tritium Gas (5000 psi, 350°C) and Aging Until Decay Helium Content Was 627 appm: (a) 100 X; and (b) 500 X. Arrow Indicates Direction of Crack Propagation.

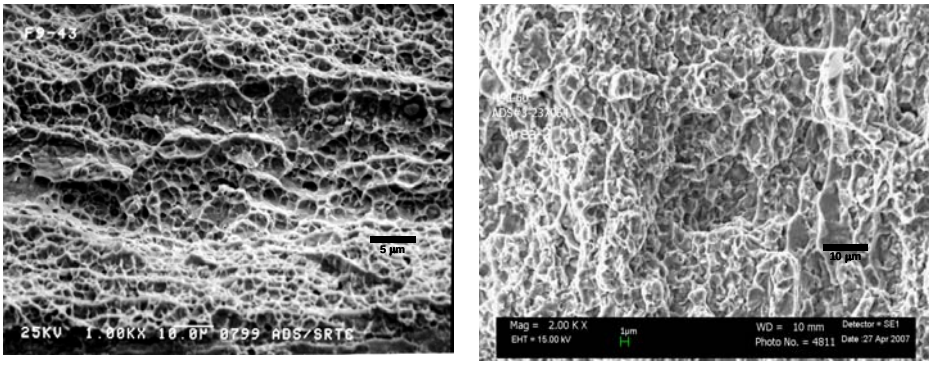

(a) ↑ **(b)** ←

Figure 15. Comparison of Fracture Appearance Between (a) Heat Treated (650°C, 24 hours) Type 21-6-9 Stainless Steel (1000 X); and, (b) Tritium-Exposed-And Aged, 627 appm helium (2000 X). Arrows Indicate Direction of Crack Propagation.

This result does not necessarily mean that all high-energy-rate-forgings are sensitized, but that there could be a potential for that to occur during forging. In fact, this study showed that sensitization heat treatments at 650°C would lower the fracture toughness values of conventional forgings just as it did for high-energy rate forgings (Figure 8). That fact that sensitization occurs in high-energy-rate forgings has been pointed out in earlier studies (12-14) and it may appear occasionally in reservoir microstructures. Furthermore, since cold work and nitrogen increase the kinetics of sensitization in Types 304L and 304LN stainless steels (15-16), these factors will increase the potential for sensitization in Type 21-6-9 stainless steel, too. The reservoir manufacturing community should be diligent in ensuring that any potential for sensitization be minimized because of its detrimental effect on fracture toughness.

The fracture toughness reductions caused by hydrogen and tritium were accompanied by changes in the size and spacing of microvoids on the fracture surface. Honeycombe (17) and Padilha (18) indicate that carbides and possibly carbo-nitrides preferentially nucleate at austenitic grain boundaries, dislocations and solute atom/vacancy clusters. Therefore, fine carbides are likely to be present throughout these as-forged microstructures. The hydrogen-exposed steels had fracture modes that were characterized by fine void sizes. This suggests that hydrogen weakens the carbide/matrix interface so much that it is easier for microvoids to nucleate on the fine carbides in the microstructure. The larger number of microvoids participating in the fracture process and their closer spacing will mean that much lower strains would be required to link up the microvoids together with the main crack. This would explain why hydrogen and tritium reduced the fracture toughness.

Tritium-exposed-and-aged steels commonly fracture by intergranular fracture. This fracture mode is results from the weakening of the grain boundary by impurities and hydrogen isotopes. Typically, the fracture surface is characterized by the absence of plastic deformation visible on the boundaries except for a few ledges and ridges produced by slip bands within the exposed grain (1, 3, and 19). The forged heats in this study were remarkably resistant to the intergranular mode of fracture, even with 800 appm helium. The fracture mode observed here is consistent with that seen in HERF tensile bars from similar heats of an earlier study (3, 20). In that study, the only samples that failed by intergranular fracture were those that were fully annealed prior to tritium exposure. A variety of substructures can evolve from the forging process (1, 15) because of either dynamic or static recrystallization. Static recrystallization, which can go to completion within a few seconds after cessation of deformation, is the dominant restoration mechanism in high-energy-rate-forged material (15). High densities of dislocations appear to limit the quantity of helium that can accumulate at a grain

boundary, where it forms pressurized bubbles and clusters that will cause an additional stress on the boundary, and reduce the cohesive area (1). Therefore, the greater the extent of recovery and recrystallization during forging or annealing after forging, the lower the dislocation density and the more the microstructure will be susceptible to intergranular fracture. More detailed transmission electron microscopy studies comparing microstructures know to fail by tritium-induced intergranular fracture and those that don't will need to be conducted to confirm this hypothesis.

Correlations between degree of sensitization and fracture toughness should be the subject of future investigations as well. These studies would be important for understanding weld heat affected zones and their degree of sensitization. However, there could be another benefit. Because fracture toughness decreases with carbide precipitation and because the fracture modes of highly sensitized stainless steel resembles tritium-induced fracture modes (Figure 15), it may be possible to develop a simulation of the helium embrittlement process by testing sensitized and hydrogen-exposed microstructures. Note that carbides preferentially precipitate at austenite grain boundaries, dislocations and on solute atom/vacancy clusters; these are similar to the sites that have decay helium bubbles in tritium-exposed-and-aged microstructures (19, 20). If a correlation between the two fracture processes could be developed, a tremendous amount of time could be saved because of the long aging times (~7 years for this study) required for studying the helium embrittlement phenomenon.

In summary, tritium and decay helium have negative effects on the fracture toughness properties of Type 21-6-9 stainless steel. Continued studies on the fracture toughness properties of stainless steels and its weldments are needed if progress can be made toward building predictive models for tritium-induced cracking. The data provide insight into the tritium compatibility of various forging processes.

CONCLUSIONS

1. High-energy-rate forged Type 21-6-9 stainless steels had lower fracture toughness values than conventionally forged stainless steels. The fracture toughness difference was attributed primarily to sensitization that occurred during the high-energy-rate forging process.

2. Hydrogen and tritium exposures lowered the fracture toughness properties of Type 21-6-9 stainless steel. The effect was manifested by lower J_Q values and lower J-da curves. The degree of sensitization did not seem to affect the fracture toughness at high decay helium levels.

3. Fracture modes of the forged steels were dominated by the dimpled rupture process in unexposed, hydrogen-exposed and tritium-exposed steels and welds. Heavily sensitized steels had a similar fracture appearance as tritium-exposed-and-aged steels

ACKNOWLEDGEMENTS

The author wishes to acknowledge the support from the U. S. Department of Energy (DOE) to the Savannah River National Laboratory (SRNL) under Contract No. DE-AC09-96SR18500.

REFERENCES

1. S. L. Robinson, B. C. Odegard, Jr., N. Y. C. Yang, D. A. Hughes, and T. Headley, "Analysis of the Microstructure and Suitability of the First Commercial Forgings For Gas Transfer System Applications, SANDIA Report, SAND99-8243, October 1999, Sandia National Laboratories, Albuquerque, NM 87185 and Livermore, CA 94550.

2. S. L. Robinson and G. J. Thomas, “Accelerated Fracture due to Tritium and Helium in 21-6-9 Stainless Steel”, *Metallurgical Transactions A*, 22A (1991), 879-885.

3. M. J. Morgan "The Effects of Hydrogen Isotopes and Helium on the Flow and Fracture Properties of 21-6-9 Stainless Steel”, *Proc. Fine Symposium*, ed. P. K. Liaw, J.R. Weertman, H. L. Marcus, and J. S. Santner, (Warrendale, PA: TMS, 1990), 105-111.

4. M. J. Morgan, M. H. Tosten, and S. L. West, “Tritium Effects on Weldment Fracture Toughness”, Savannah River National Laboratory, WSRC-STI-00056, July 17 2006.

5. M. H. Tosten and M. J. Morgan, “Microstructural Study of Fusion Welds in 304L and 21Cr-6Ni-9Mn Stainless Steels (U)”, WSRC-TR-2004-00456, March, 2005

6. M. H. Tosten and M. J. Morgan, “Transmission Electron Microscopy Study of Helium-Bearing Fusion Welds”, WSRC-TR-2005-00477, November, 2005.

7. M. J. Morgan and M. H. Tosten, "Microstructure and Yield Strength Effects on Hydrogen and Tritium Induced Cracking in HERF Stainless Steel", *Hydrogen Effects on Material Behavior*, ed. N. R. Moody and A. W. Thompson, (Warrendale, PA: TMS, 1990), 447-457.

8. ASTM E647-95a “Standard Test Method for Measurement of Fatigue Crack Growth Rates” *1999 Annual Book of ASTM Standard Volume 3.01 Metals-Mechanical Testing; Elevated and Low-Temperature Tests; Metallography*, American Society for Testing and Materials, 1999.

9. ASTM E1820-99 “Standard Test Method for Measurement of Fracture Toughness”, *1999 Annual Book of ASTM Standard Volume 3.01 Metals-Mechanical Testing; Elevated and Low-Temperature Tests; Metallography*, American Society for Testing and Materials, 1999.

10. T. L. Anderson, *Fracture Mechanics Fundamentals and Applications*, CRC Press LLC, 1995, pp. 265-281.

11. ASTM E399 “Standard Test Method for Plane-Strain Fracture Toughness of Metallic Materials”, *1999 Annual Book of ASTM Standard Volume 3.01 Metals-Mechanical Testing; Elevated and Low-Temperature Tests; Metallography*, American Society for Testing and Materials, 1999.

12. E. C. Sanderson, A. W. Brewer, R. W. Krenzer, G. Krauss, “Dislocation Substructures in High-Energy-Rate-Forged and Press-Formed 21-6-9 Stainless Steel”, Rockwell International Atomics International Division, Rocky Flats Plant, P. O. Box 464, Golden, CO 80401, RFP-2743, July 24, 1978.

13. M. C. Mataya, M. J. Carr, R. W. Krenzer, and G. Krauss, “Processing and Structure of High Energy Rate Forged 21-6-9 and 304L Forgings, Rockwell International Atomics International Division, Rocky Flats Plant, P. O. Box 464, Golden, CO 80401, MTGM-80-59.

14. M. C. Mataya, E. L. Brown, and M. P. Riendeau, “Effect of Hot Working on Structure and Strength of Type 304L Austenitic Stainless Steel, Metallurgical Transactions A, Volume 21A (1990) pp. 1969-1987.

15. J. O'Donnell, H. Huthmann, and A. A. Tavassoli, "The Fracture Toughness Behavior of Austenitic Steels and Weld Metal Including the Effects of Thermal Aging and Irradiation", *Int. J. Pres. Ves. & Piping*, 65 (1996), 209-220.

16. V. Kain, K. Chandra, K. N. Adhe, P.K. De, "Effect of Cold Work on Low-Temperature Sensitization Behavior of Austenitic Stainless Steels", *Journal of Nuclear Materials*, 334 (2004), 115-132.

17. R. W. K. Honeycombe, *Steels Microstructure and Properties* (Metals Park, Ohio) ASM 1981.211-235.

18. A. F. Padilha and P. R. Rios, "Decomposition of Austenite in Austenitic Stainless Steels" ISIJ International, Vol. 42 (2002), No. 4, pp. 325-337.

19. M. J. Morgan and M. H. Tosten, "Tritium and Decay Helium Effects on the Fracture Toughness Properties of Types 316L, 304L, and 21Cr-6Ni-9Mn Stainless Steels", *Hydrogen Effects in Materials*, ed. A. W. Thompson and N. R. Moody, (Warrendale, PA: TMS, 1996), p. 873.

20. M. H. Tosten and M. J. Morgan, "The Effects of Helium Bubble Microstructure on Ductility in Annealed and HERF 21Cr-6Ni-9Mn Stainless Steel", WSRC-TR-92-551, February, 1998.